The chronology of Insiza cluster Khami-phase sites in south-western Zimbabwe: compositional insights from pXRF and Raman analysis of excavated exotic glass finds

F. Koleini[1], L. H. Machiridza[2], I. Pikirayi[1] and Ph. Colomban[3]

[1] *Department of Anthropology and Archaeology, Faculty of Humanities, University of Pretoria, Pretoria, Gauteng, South Africa.*
[2]*Department of History, Archaeology and Development Studies, School of Arts, Culture and Heritage Studies, Great Zimbabwe University, Masvingo, Masvingo, Zimbabwe*
[3] *Sorbonne Université, CNRS, MONARIS UMR8233, 4 Place Jussieu, 75005 Paris, France*

ABSTRACT

Fourteen glass beads and one glass fragment from Khami-period (AD 1400-1830) sites of Danamombe, Naletale, Gomoremhiko, Nharire and Zinjanja in Zimbabwe, were analysed by pXRF and Raman spectroscopy with the intention to correlate the results with associated radiocarbon dates. The results show that Zinjanja and an earlier part of Danamombe stratigraphic context had Khami Indo-Pacific beads (15th-17th centuries) corresponding with Torwa occupational layers. Other European beads and one bottle fragment (HLLA-glass) dating from the 16th to the 19th centuries were confined to the top stratigraphic layers of Danamombe and Naletale, which coincide with the later Rozvi occupational layers. Gomoremhiko had one Mapungubwe-Zimbabwe bead series (13th-15th centuries), which suggests that it was probably earlier than the other sites. All European beads are made of soda-lime plant-ash glass with high alumina that makes them comparable with glass produced through the Mediterranean traditions in southern Europe.

Key words: Post European trade, Glass beads, Khami-phase, Rozvi, Torwa, pXRF, Raman

INTRODUCTION

This study pays special attention to the Khami-phase stone-building tradition, which is distributed on the Zimbabwe plateau and adjacent regions of north-eastern Botswana and northern parts of South Africa around the Soutpansberg area (Chirikure et al. 2014). Chronologically, the Khami-phase (AD 1400-1830) constitutes the third phase of the Zimbabwe Culture. The Zimbabwe Culture is divided into three broad archaeological and architectural sequences, namely Mapungubwe (AD 1220-1290), Zimbabwe (AD 1300-1550), and Khami (AD 1400-1830) (Huffman 1996; Pikirayi 2001).

Although the Khami-phase has recently begun to attract renewed academic interest as part of the ongoing Zimbabwe Culture debate, its detailed chronology remains poorly known (Chirikure et al. 2017). Archaeologists lack basic information on the chronology of key sites, especially those associated with both Torwa and Rozvi dynasties in the south-central parts of the Zimbabwe plateau. As such, a cluster of Khami-phase sites consisting of Danamombe, Naletale, Gomoremhiko and Zinjanja (see Fig. 1) were re-examined in order to ascertain their chronological development based on radiocarbon dating and historically dateable imported artefact (Fig.2). This chronological data was crucial in assigning archaeological identities on the Torwa and Rozvi dynasties, who once lived in these settlements (Beach 1980; Machiridza 2005, Machiridza 2012; Mudenge 1988; Pikirayi 2001).

The Torwa ruled these sites from the fifteenth century until AD 1644. Sometime between AD 1685 and 1696, Rozvi dynasties from north-eastern Zimbabwe took over control of the centres assimilating, the fragmented Torwa until they were also defeated by the Ndebele during the 1830s (Beach 1980; Mudenge 1988). While a lot is known historically about

Rozvi origins and their eventual assimilation of the Torwa population in south-western Zimbabwe, it remains difficult to archaeologically establish Rozvi identities or their role in the development of Danamombe and related smaller sites in south-central Zimbabwe (see Burrett 1998; Garlake 1973; Machiridza 2012; Pikirayi 2001).

It is worth noting that both systematic and random excavations previously conducted at the sites of Danamombe, Naletale and Zinjanja yielded large quantities of glass beads thereby proving that international trade was quite common in the Zimbabwean plateau interior and beyond (see Burret 1998; Caton-Thompson 1931; Hall and Neal 1904; Machiridza 2012; Randall-MacIver 1906; Summers 1971). Danamombe has so far yielded the largest number of glass bead owing to its historical stature as a state capital (see Caton-Thompson 1931; Randall-MacIver 1906). While most of these excavated beads are available at the museum of Human Sciences in Harare, they lack clear archaeological context. This made it impossible to correlate the museum collection to the recently recovered sample of glass beads.

The trade in glass beads in southern Africa stretches as far back as the 7th century AD (Wood et al. 2012). From this period onwards, beads from the Middle East (7-10th centuries) and later, from the south and south-eastern Asia (mid10-17th centuries) were introduced into the region (Robertshaw et al. 2010). After the arrival of European traders which coincided with developing of Khami phase sites and the demise of Swahili trade in eastern and southern Africa, Asian beads were gradually replaced by European beads. In the beginning (15th century), the Portuguese imported beads from southern Asia to eastern and southern Africa (Wood 2011). These are the beads recovered from Khami-phase sites and categorized as belonging to the Khami Indo-Pacific (Khami-IP) series (Wood 2009; Wood 2011; Robertshaw and Wood 2017; Koleini et al. 2017b).

Glass beads along with other trading goods were transported via the Indian Ocean trade route and distributed into the hinterlands from ancient ports situated along the east coast of Africa. Detailed compositional study by Robertshaw et al. (2010) and visual description by Wood (2011) show that glass beads can be used as chronological markers especially when classified according to morphology and composition (see Table S1). Later studies of glass beads using Raman spectroscopy also identified pigments and opacifiers that some are chronological markers (Prinsloo and Colomban 2008; Prinsloo et al. 2011; Koleini et al. 2016a).

Recent studies of glass beads conducted through the aid of a combination of pXRF and Raman spectroscopy demonstrated the efficiency of these mobile techniques in defining the chronological sequences of traded glass bead series in southern Africa (Koleini et al. 2016a, 2016b; Koleini et al. 2017a; Koleini et al. 2017b). Following the method reported in Koleini et al. (2016b), the glass beads analysed in this paper are first classified morphologically (see Wood 2011) and then subjected to pXRF and Raman spectroscopy to reveal links between material culture and the date of their contexts. The results are then compared to archaeological sites elsewhere in Zimbabwe (Baranda), Botswana (Basinghal Farm) and South Africa (Magoro Hill) where similar beads series were recovered (Koleini et al. 2016a, 2016b; Koleini et al. 2017b).

INSTRUMENTS AND METHODS

pXRF measurements

A portable Niton Thermo Scientific XL3t GOLDD was used for XRF analysis of the beads (for further details, see Koleini et al. 2016a). The samples are examined using fundamental

calibration parameters used in mining Cu/Zn mode. Four elemental ranges, main, low, high and light with measurement duration of 240 seconds in total were selected. Semi-quantitative result for the concentration of 36 elements excluded sodium that cannot be detected due its low-Z was reported in ppm by the device software. Afterwards, the results were converted to oxide (wt%) of elements and normalized.

That portable XRF instruments can be inaccurate in quantitative measurements of elements. This inaccuracy is related to instrumental restrictions and intrinsic characteristics of archaeological samples. The measurement is first affected by the limitation in quantification of low-Z elements due to the strong absorption of X-ray by air, spectral interference of elements and the calibration of instruments, which were not specifically designed for analysis of archaeological samples (Hunt and Speakman 2015). These restrictions make analysis of reference samples a necessity for estimating the accuracy of measurements and designing a policy for the classification of the beads.

The second restriction is due to the non-invasive approach in analyzing of archaeological samples: due to the variable shape of the objects, the distance between the instrument and the sample is not constant. However, non-invasive techniques are now preferred or even mandatory from a conservation point of view. Normalisation with a common major element such as silicon (see e.g. Simsek et al. 2014) or with the cathode signal waives this problem for the composition comparison. Contrary to destructive techniques such as LA-ICP-MS that destroy the upper surface of the sample, the small and variable penetration of X-ray beam can be affected by the presence of a corroded/lixiviated surface glass layer, which is depleted in alkali/earth-alkali ions, i.e. enriched in silica (Tournié et al. 2008).

In order to evaluate the problems, some of the analysed glass beads with LA-ICP-MS by Robertshaw et al. (2010) were examined by pXRF as 'reference samples' and the results were compared (see Table S2, this paper; Koleini et al. 2016a). The beads dated from the 10th to the 17th centuries and consist of K2, Khami Indo-Pacific (mineral soda glass), Mapungubwe and Zimbabwe series (plant-ash glass) that are preserved in van Riet Lowe collection at the University of the Witwatersrand. Although the results are not exactly the same as the outcome of LA-ICP-MS, they show the same tendency in the concentrations of the main 6 glass oxides and uranium in the bead series. The differences in the results might reflect the surface lixiviation of the glass beads and the absence of soda concentration. The advantage of this measurement is that the reference data was collected from samples with the same morphology and close composition as the study samples.

In this paper, we chose analysis of the glass samples B and D of the Corning museum of glass as a reference for classification of the glass beads discovered from the Khami-phase sites of Danamombe, Naletale and Zinjanja. In order to estimate the precision of the results, the Corning reference glass samples B and D were each analysed three times. The results were then converted to oxides form and averaged for comparison with certified values (Table S3). The reference samples are replicas of ancient glasses and their compositions reported in Brill (1999). Sample B is a soda-lime silica glass with low magnesium content and sample D is a potash lime glass.

The XRF results show that silica is higher than the certified value in both samples and the amounts of potash and lime are slightly lower in sample D. However, the ratio of potash to lime is equal for the two instruments. The rest of the oxides concentrations are very close to the certified values that show reliability of pXRF in detection of these glass types. The

deviation of pXRF results from certified values was corrected with the impact of normalization factor (NF) obtained by measuring the ratio of certified value to the recorded value. Due to unavailability of sample A (soda-lime glass with magnesia content), the average NF of samples B and D was used for the correction of plant-ash glasses results.

Raman spectroscopy

Raman spectroscopy was performed by the use of a T64000 micro-Raman spectrometer (HORIBA JobinYvon, France). The Raman spectra were excited with the 514.5 nm lines of a Krypton Argon mixed gas laser that was focused on the surface with a 50x objective. Typically, the volume probed is 5x5x15 μm^3 and the focus is adapted to get the stronger signal arising from preserved, dense glass. Because of the porosity of the lixiviated surface, the Raman signature is weaker and its contribution to the spectrum limited. One spectrum with the baseline correction from 400 cm^{-1} was recorded by a portable HE532 (Horiba JobinYvon, France) spectrometer. The details of instruments, recording procedures and enhancing the spectra by baseline correction is found in Koleini et al. (2016b).

SITES AND SAMPLES MORPHOLOGY

Danamombe

Danamombe (Dhlodhlo) an elite dry stone-walled platform, elaborately decorated and surrounded by a few isolated enclosures built is rough walling is one of the most important Khami-phase settlements. This site is situated in central Zimbabwe about 86 km south-west of Gweru city and it spreads over an area of 1.2 km^2. The Torwa are reported in oral accounts

as the first rulers to occupy this site (see Machiridza 2013; Posselt 1935; van Waarden 2012). Later on, the Rozvi people, who migrated from the north-east eventually occupied Danamombe and made it their capital from the 1690s up until the 1830s (Beach 1980; Huffman 1996; Pikirayi 2001).

Three locations defined by Trench I, Test Pits I and II (Fig. S1) were selected for excavation at the site. Trench I and Test Pit II comprise traded glass beads. Only one olive vessel fragment was found in Test Pit I (see Table S4). Radiocarbon dates assign Trench I to a period between the early 15th and 20th (D-AMS025194, D-AMS025195, D-AMS025196). For detailed summary of radiocarbon dates from the sites see Table S5.

Trench I was 3.25 m deep yielding a total of 13 glass beads. Five of these beads were heavily charred to the extent that glass composition and morphology could not be used to classify them. Four brownish-red, two dark blue and one white bead were selected for classification (Fig. 2). All the beads were manufactured using the drawn technique. Among the selected beads, one dark blue bead (DAN16) found in layer 12 is morphologically attributed to the Khami series (15th-17th centuries) (see Table S4).

The rest of the beads are probably of European origin. Three brownish-red on black are compound (two layers) in structure, and bear resemblances with Indian red on green (IROG) (Wood 2008). These beads were produced in Europe and imported to Africa from the 18th to 19th centuries (Caton-Thompson 1931; Beck, in Caton-Thompson 1970).

Three glass beads discovered in Test Pit II are all morphologically European in terms of origin (Table S4). The beads are dark blue and one is white. Despite the proximity of this

Test Pit to Trench (I), no brownish-red beads were found here.

Naletale, Gomoremhiko and Nharire Hill

Naletale is widely cited in oral traditions as one of the former Rozvi capital sites (Burrett 1998; Huffman 1996; Machiridza 2012). This site is located some 25 km northeast of Danamombe. Gomoremhiko and Nharire hills are sites situated south-east and south-west of Naletale respectively. Excavations were later extended to Gomoremhiko and Nharire hill, treated in this research as satellite sites to Naletale, to further understand the latter through related material culture and chronometric dates. The recently excavated Test Pit II at Naletale main platform shows three phases of occupation. Radiocarbon dates from this Test Pit indicates that Naletale dates from the middle of the 17th century to the middle of 20th century (D-AMS024217, D-AMS024218, D-AMS024219) (see Tables S5).

One white and one blue-green glass beads were found at Nharire hill and Gomoremhiko respectively. The blue-green glass bead from Gomoremhiko is similar morphologically to Mapungubwe and Zimbabwe bead series dating between 13th and 15th centuries while the large white bead from Nharire hill is European dating to the late 16th century (Francis 1992) (Table S4). Based on this evidence, Gomoremhiko is probably earlier in date than Naletale main settlement and Nharire hill.

Zinjanja

Zinjanja (Regina) is yet another Khami-phase site widely documented in oral traditions as a former Rozvi capital (Huffman 1996; Machiridza 2012; Pikirayi 2001; van Waarden 2012).

This site is situated 90 km southwest of the town of Gweru, in South-central Zimbabwe. Radiocarbon dates that were derived from Test Pits II and III situated on a midden about 50 m north of the main platform suggest that this part of the site was occupied between the 17th and early 20th centuries (D-AMS024220, D-AMS024221) (Table S5). A much tighter chronology comes from van Waarden (2012:100) whose radiocarbon dates places Zinjanja between AD 1649 and 1673.

A single fragile yellow bead, which later fragmented during the course of cleaning, and two other beads with light and dark blue colours were recovered from the midden excavations (Fig. 2). After a consideration of their morphological attributes, these beads were classified as Khami-IP series (Table S4).

RESULTS

Glass composition

The major and minor elemental oxides concentration (wt%) of glass beads are presented in Table 1. The results show that all the beads are soda-lime silica glass with sand as the source of silica. None of these beads were made of pure quartz or flint pebbles due to a high concentration of alumina (>3 wt%) in the composition. The beads were then divided into 4 groups based on the concentration of aluminium, calcium and potassium oxides that were plotted against each other (Fig. 3). Based on XRF results, only 7 samples were selected for Raman spectroscopy and beads with the same composition were not analysed.

Figure 4 shows representative spectra of glass matrix and pigments. When the bead is

coloured with a pigment, i.e. forms a glass-ceramic, the spectrum of the pigment superimposes on to that of the glassy matrix (Fig. 4b, spectrum #2) and even dominates (Fig. 4b, spectra #1 & 3). The Raman classification of glass is performed by plotting of the peak maxima (wavenumber cm^{-1}) in bending (500 cm^{-1}) versus stretching (1000 cm^{-1}) broad vibration bands of SiO_4. This abacus reflects the perturbation of the SiO_4 tetrahedron with adjacent ions (sodium, potassium, lead, calcium) and polymerisation degree (Colomban 2003; Mysen and Richet 2005). This allows visual identification of glass types by using glass matrix spectra (Fig. 5). The method was formerly used to classify southern African beads recovered at K2, Mapungubwe Hill, Basinghall Farm, Mutamba, Magoro Hill and Baranda (Tournié et al. 2012; Koleini et al. 2016a, 2016b; Koleini et al. 2017a; Koleini et al. 2017b). The results of XRF and Raman measurements can be summarized as follows:

Group 1: The first group is a mineral soda glass with high alumina (>7.9 wt%) and low magnesia (<1 wt%). The uranium oxide content is between 48 and 121 ppm and only detected in the beads in this group. This composition makes the beads similar to those of the Indo-Pacific series. Figure 3 shows that concentrations of alumina, lime and potash in these beads are quite similar to Khami-IP series that were found in Basinghall Farm (mid-11th to mid-17th centuries), Baranda (16th to 17th centuries) and Magoro Hill (18th to 19th centuries).

The beads found at Zinjanja (Zin1-3) and one from Danamombe (DAN16) fall into this group. Raman measurement of a representative bead, DAN16, shows the typical spectrum of Khami series that placed it in the soda cluster (Fig. 4a, spectrum #1, Fig. 5, group A) (Koleini et al. 2017b). The samples in this group exhibit a strong component around 450-500 cm^{-1} in bending and 1070-1100 cm^{-1} in stretching bands. Group A consists of K2, East Coast and

Khami-IP series that were manufactured in south Asia in addition to some European beads. Khami series generally contains higher lime and iron than the East Coast and K2-IP series (Koleini *et al*. 2016b).

Group 2: The second group contains lower alumina (3.2-6 wt%) and higher lime (7-11.8 wt%) and magnesia (>1.5wt %) compared to Khami-IP series. Consequently, these beads are assigned to the European plant-ash, soda-lime-silica type. The alumina content is remarkably high for most of the European plant-ash glass manufactured after the 10th century AD except those that were manufactured in Italy, Spain and Portugal (Cagno et al. 2010; Coutinho 2016; de Juan Ares and Schibille 2017). The glasses in these regions were manufactured by using local high impurity sand and plant-ash from the Levant, Spain, France and Tunisia (Malandra 1983). The result is a glass with more than 3.5 wt% alumina.

The potash content of beads in this group is in a range between 3.9 and 6 wt% that put the beads in two categories of flux type (Fig. 3). One category with low potash (<4 wt%) is the typical of glass made by using Levantine ash and the second category with high potash (>4.5 wt%) is the typical of glasses made of Barilla ash, from the West Meditterranean (Barrera and Velde 1989). DAN4 and 11 contain potash close to Levantine ash and the rest of beads (DAN6, 9, 12, 13 and NHA1) were manufactured with potash close to Barilla ash.

A mixture of sand and Levantine ash in the manufacture of glass reported from sites dated from the 10th century to the 16th century in Ciudad de Vascos (Spain), Silves (Portugal), Tuscan and Savona (Italy) (Cagno et al. 2010; Cagno et al. 2012; de Juan Ares and Schibille 2017). Among these sites, samples from Vascos are earlier (mid-11th century to early 12th century) than this assemblage. Barilla (west Mediterranean ash) in a mixture with sand was

reported in the production of glass in Tuscany (16th century) and Savona (13th -16th centuries) in Italy (Cagno et al. 2010; Cagno et al. 2012) (See Table S6).

There are also glass samples with high (within 3-6 wt%) and very high alumina (>6 wt%) from Coimbra and Tarouca in Portugal dated to the 17th century, and made of Barilla and Levantine ash (Lima et al. 2012; Coutinho 2016). These glasses were manufactured with soda-rich flux following Mediterranean traditions (Coutinho 2016). However, no glass beads were found or reported from the above-mentioned sites. Among imported glass beads brought to southern Africa, same compositions were reported for some European beads found in Magoro Hill (Fig. 3).

Raman measurements on DAN12 and NHA1 (Barilla ash) and DAN6 (Levantine ash) placed them in the soda/lime cluster with the general spectrum #2 and #3 respectively (Fig. 4a). The spectra show peak maxima around 540-650 cm^{-1} in bending and 1070-110 cm^{-1} in stretching bands (Fig. 5, group B).

Group 3: The third group of samples contains alumina and lime levels at the intermediate of Khami-IP and European beads of the second group. High alumina content (>8.7 wt%) is consistent with the use of river sand as source of silica, typical for soda-lime-silica glass of south and south-eastern Asia (Robertshaw et al. 2010). Lime less than 7.5 wt% indicates the use of a different type of plant-ash or sand with low content calcium compared with the second group. This composition is the typical plant-ash glass of south-eastern Asia (Robertshaw et al. 2010). Plant-ash soda-lime glass of Mapungubwe and Zimbabwe series as well as some European beads are placed in this group (Koleini et al. 2016a). The discrimination between these European beads and Mapungubwe and Zimbabwe series is only

possible by considering the morphology and opacifiers in the beads.

Three beads from Danamombe (DAN2, DAN7, DAN14) are included here. From these, DAN2 and DAN14 have a corroded surface with a total depletion of magnesium and certainly, loss of potassium, the easier lixiviated ion (Tournié, Ricciardi and Colomban 2008) and they are not considered in this classification. One minute blue-green bead classified as Mapungubwe-Zimbabwe series (MH1) was also included in this group.

Raman measurements on MH1 and DAN7 recorded the typical Raman spectrum #3 in Figure 4a. As a result, these beads, which are the same as beads in the second group, were placed in the soda-lime cluster (Fig. 5, group B). A wide range of soda-lime glasses with diverse soda (10-20 wt%) and lime (8-16 wt%) concentrations have been placed in this cluster (Tournié et al. 2012). These glasses can be discriminated by the shape of the stretching band in their spectra (Fig 4a, spectra #2 and 3) (Tournié et al. 2012; Koleini et al. 2016b). Differences in the shape of bending and stretching bands (peak position, intensity and wideness) can be attributed to the composition and the production temperature (Colomban et al. 2003).

Group 4: The fourth group is limited to one sample, a vessel fragment, DAN1, with alumina in the range of European beads (<6 wt%) in group 2. The fragment contains high levels of lime (24 wt%) and low potash (2 wt%) that makes it close to European greenish high lime low alkali glass (HLLA). HLLA glass was produced by using plant-ash yielded from burning a wide variety of wood and plant species (Schalm et al. 2007, Dungworth 2011).

In general, HLLA glass could be classified based on soda, P_2O_5 and MnO_2. Soda is not detectable with pXRF, and therefore, it was impossible to compare the soda content of DAN1

with HLLA glasses from different parts in Europe. Except P_2O_5 concentration which is high in DAN1 (1.38 wt%), the rest of elemental concentrations are very close to the HLLA samples found in Savona (15th-16th centuries), north of Italy (Cagno et al. 2012). High P_2O_5 (1.4 wt%) make the flux very close to unpurified wood ash.

Raman spectrum of DAN1 is completely different from the rest of spectra with high intensity bending and stretching peaks at 610 cm^{-1} and 945 cm^{-1} (Fig. 4a, spectrum #4). As the result, the sample was placed in the lime/potash cluster (D) in Figure 5 as reported by Ricciardi et al. (2009).

Pigments and colorants

Two types of pigments have been identified: pyrochlore solid solution ($Pb_2Sb_{2-x-y}Sn_xM_yO_{7-\delta}$, M= Fe, Zn, Si…), also called Naples Yellow, and $Ca_2Sb_2O_7$ white opacifier (Fig. 4b) (Ricciardi et al 2009). These pigments are used since Roman times and typical of Mediterranean productions. While lead tin yellow type (II) was detected in European and pre-European bead series in southern Africa, calcium antimony was only found in European series that were imported from the late 17th until 19th centuries (Hancock et al. 1997). The other colouring agents are metallic ions dissolved in the glassy matrix (Cu^{2+}, Co^{2+}, Fe^{3+}). The identified colorants and pigments in the samples are listed in Table S4.

Among the beads, ZIN3 that was classified in Khami series, contains a combination of lead and tin, in the form of lead tin yellow type (II) (Fig. 4b, spectra #1). The combination of lead tin yellow (II) and copper ions forms the blue-green colour in (MHI1) that was classified in Zimbabwe bead series. The green colour of DAN1 is due to Fe^{3+} ion. The white colour of

DAN2, DAN11 and NHA1 is due to the presence of antimony ($Ca_2Sb_2O_7$) in the composition (Fig. 4b, spectrum #2). Antimony has the role of white pigments in some of European beads with the same glass composition found in Magoro Hill (Koleini et al. 2016).

The Khami light blue bead (ZIN2) was coloured with copper ions. The bead also shows anatase (TiO_2) as impurity in the composition (Fig. 4b spectrum #3). Anatase is a very common impurity of clays and river sand.

All the brownish-red beads of this assemblage are coloured with a combination of iron and copper ions. Iron acts as a reducing agent for precipitation of copper ions in its atomic form (Ricciardi et al. 2009), with Cu° metal being a very efficient colouring agent at very low level. Minor oxides of antimony and manganese make the colorants close to IROG beads found at Garumele (17-18th century) in Niger (Robertshaw et al. 2014). However, the glass composition of Danamombe brownish-red on black except one bead (DAN9) are different from Garumele beads by their higher concentration of alumina. Copper as a red colorant was found in most of the red beads in southern Africa dating from 1000 AD, and thus it seems the colorant is of no specific chronological value.

Dark blue beads were coloured with cobalt oxide. The concentration of Arsenic in Khami beads is lower (Co/As>0.5) than in European beads (Co/As<0.4) indicating at least two different sources/processes. Cobalt in European Danamombe beads regarding traces of Ni (<280ppm) is close to that measured in Garumele and some of Magoro beads with the same glass composition (Robertshaw et al. 2014; Koleini et al. 2016a). The composition of the ores are assumed smaltite or erythrite of Schneeberg mines in the eastern parts of Germany (Gratuze et al. 1992).

DISCUSSION AND CONCLUSION

The morphological and chemical analysis of glass beads and the single glass fragment coupled with radiocarbon dates enhances our appreciation of the chronology of the sites highlighted above. The results show that the majority of the analysed beads except for just five samples were of clearly European origin (Table S4). Four beads belong to the Khami series manufactured by mineral soda glass with high alumina comparable with south Asia glass (Robertshaw et al. 2010). Portuguese traders imported Khami beads into southern Africa between the 15th and 17th centuries due to the native people's bias towards imported glass beads from Asia (Axelson 1973; Wood et al. 2009; Wood 2011).

Table S4 shows that only a single Khami bead series was found at Danamombe (Tr1-Lv12) while the rest of the layers above contained post-17th century European beads based on morphology and/or pigments. This supports the hypothesis that the lower layers are earlier than the upper/top layers. The European beads samples dominating the top layers consist of brownish-red on black beads, white beads coloured with calcium antimoniate and cobalt blue beads.

The compound brownish-red on black beads were imported into Africa between the 18th and 19th centuries and calcium antimoniate white beads are dated from the late 17th to 19th centuries (Beck, in Caton-Thompson 1970; Caton-Thompson 1931; Tournié et al. 2012). In cobalt blue beads, the associated elements (Ni and As) with cobalt indicates the use of cobalt from Schneeberg mines in Germany that was in use from the 16th to18th centuries (Gratuze et al. 1992).

All these European beads are believed to date from the late 17th century onwards. Therefore, it is most likely that they were all imported during the late 17th to the late 18th centuries. After this date, from the late 18th century, lead arsenate was widely used in the manufacture of glass beads (Hancock et al. 1997). However, none of the beads had lead arsenate at both Danamombe and its cluster sites.

The only sample from Danamombe Test Pit I is a HLLA glass that was largely manufactured during the post-medieval to early 18th century in Europe. Test Pit II contains any Khami series beads and finds are restricted to cobalt blue and white European beads that are similar to beads from Trench I in terms of composition. In conclusion, Test Pit I and II are characteristic of the latter occupation phase of Danamombe (late 17th to late18th centuries). The rest of Khami series beads (3) were found at Zinjanja, which shows that this site was also contemporary with the early occupation phases of Danamombe (15th to 17th centuries). The one oyster white bead of Naletale (Nharire Hill) coloured with calcium antimony therefore has the same date as white European beads from Danamombe. The blue-green bead found at Gomoremhiko has a similar composition to Mapungubwe and Zimbabwe beads (13th-15th centuries) but its uniqueness prevents a firm conclusion that this site was earlier than the rest of the sites under study.

All the European beads contain high alumina content that makes them different from the glass of central and western Europe with less than 3 wt% alumina (Table S6). High alumina content of the beads in this assemblage indicates that most of the beads were probably manufactured in one of the southern European countries (Italy and Portugal) where local high alumina sand was used in the production of glass.

Low potash (<4 wt%) makes the flux in the production of three beads from Danamombe close to Levantine ash, a soda-rich ash made of burning soda-rich coastal plants (eg. *Salsola*). There is evidence of importing Levantine ash to southern Europe from the 6th to the 16th centuries (Cagno et al 2010; Cagno et al. 2012). The use of Levantine ash gradually decreased during the 17th century. High potash (>4.5 wt%) in four Danamombe and one Naletale beads makes the used flux in their production close to the west Mediterranean local soda-rich ashes (e.g. Barilla).

Levantine ash was substituted by the west Mediterranean ashes from the mid-16th century, and were widely used in the production of soda glass until the end of the 19th century (Velde 2013; Coutinho 2016). Close mixtures of local sand and ashes from Levantine and west Mediterranean were reported from Silves, Coimbra and Tarouca (Portugal), Tuscan and Savona (Italy) (Cagno et al. 2010; Cagno et al. 2012; de Juan Ares and Schibille 2017). Based on available data (composition and date) the European beads of this assemblage (group 2) are more close to Tuscan, Savona, Coimbra and Tarouca glasses while more accurate measurements of trace elements are necessary for finding the exact source of the beads.

Among the European beads, some have alumina content very close to high alumina plant-ash glass of south Asia such as Mapungubwe and Zimbabwe series while the identified pigment and morphology indicates the beads are European. No clear source for these beads was identified.

Although a low number of beads were recovered through recent fieldwork, the distribution of the identified bead series in layers was quite representative. The small sample of glass beads recovered from recent excavations was conditioned by the nature of sites selected for

study, excavation objectives and the general location of excavation units. For instance, Gomoremhiko and Nharire hill were regarded as satellite sites of Naletale. Excavations done around these zones were characterised by very shallow cultural deposits that however helped in confirming the chronology of Naletale main platform. In fact, the main platforms found at Danamombe, Naletale and Zinjanja were largely meant for elite occupation, hence they are generally clean if not devoid of large amounts of cultural finds. These artificial platforms were primarily targeted for their potential to yield dateable material in sealed contexts. The associated nearby middens were only excavated to enhance inferences on main platform occupational sequences. As such, the small sample of glass beads recovered, coupled with radiocarbon samples, offered unique opportunities to accurately determine the chronological development of each settlement.

Furthermore, the small sample of glass beads analysed above corroborates oral and documentary sources relating to Khami-phase sites in several ways. While the chemical properties of these beads do not directly symbolise Torwa and Rozvi identities, they chronologically distinguish the Torwa (~1400-1644) from Rozvi (~1685-1830) occupational phases. It appears the Torwa traded more in Khami series beads than European ones, while the Rozvi enjoyed access to both Khami series and European beads.

These trends should be understood in the context of shifts in bead production from the source markets and African ethnic or political group preferences (see Bhatt 2016:19-20). As such, when Portuguese traders arrived to replace the Swahili traders from the 15th century onwards, they had to first respect African preferences before they gradually introduced European beads that characterise the upper/top occupational layers at the selected Khami-phase sites. Since we know the Rozvi were the last historical dynasties to rule from the

research sites, we can as well posit that glass beads falling within the upper/top occupational layers generally coincided with Rozvi period of governance. However, the earlier Mapungubwe/Zimbabwe series beads (13th-15th centuries) and Khami series beads (15th-17th centuries) still continued in circulation although they were being gradually phased out in favour of the incoming European beads as demonstrated by their distribution at the three research sites.

Glass bead variation and associated radiocarbon dates alone are not enough to distinguish the Torwa from the Rozvi occupation of these sites. However, they can at least signify two separate occupational periods at the selected Khami-phase sites namely; an earlier (15th to 17th century) and later (17th to 20th century) period. These periods coincide with the reign of both Torwa and Rozvi dynastic groups. As such, Torwa occupational layers were characterised by Khami bead series and probably some Mapungubwe/Zimbabwe beads. In contrast, Rozvi occupational layers were characterised by samples of both Khami and European beads series. These distributional patterns may reflect regional trends in trade, whereby Portuguese arrived much later and introduced European bead varieties that gradually replaced bead varieties from south Asia. Interestingly, bead (size and colour) attributes basically remained the same (save for white beads). More so, radiocarbon dates from these Khami-phase sites are in agreement with the dates of manufacture of the associated glass beads and green bottle fragment.

ACKNOWLEDGMENTS

The authors wish to thank, Stephen P. Koob and Corning Museum of glass for supplying the standard glass samples. Farahnaz Koleini and Innocent Pikirayi acknowledge the financial

contribution from the National Research Foundation of South Africa, through the research project Great Zimbabwe's Complexity, Competitive Support for Rated Researchers, grant no. N105866.

REFERENCES

Axelson, E., 1973, *The Portuguese in South-East Africa 1488-1600*, Struik, Johannesburg.

Beach, D. N., 1980, *The Shona and Zimbabwe 1900-1850.* Mambo Press, Gweru.

Bhatt, M., 2016, Bead and Beadwork Traditions: A study of Trade and Cultural Exchanges across the Coast of Gujarat, East Africa and the Red Sea, *Textile Society of America Symposium Proceedings*, 965, 17-26.

Burrett, R. S. 1998, Naletale: A Khami type settlement near Gweru, *Heritage Zimbabwe*, 17, 138-150.

Cagno, S., Mendera, M., Jeffries, T., and Janssens, K., 2010, Raw materials for medieval to post-medieval Tuscan glassmaking: new insight from LA-ICP-MS analyses, *Journal of Archaeological Science*, 37, 3030-3036.

Cagno S., Brondi Badano M., Mathis F., Strivay D., and Janssens K., 2012, Study of medieval glass fragments from Savona (Italy) and their relation with the glass produced in Altare, *Journal of Archaeological Science*, 39, 2191-2197.

Caton-Thompson, G., 1931, *The Zimbabwe Culture*, Clarendon Press, Oxford.

Chirikure, S., Manyanga, M., Pollard, A. M., Bandama, F., Mahachi, G. and Pikirayi, I. 2014, Zimbabwe culture before Mapungubwe: new evidence from Mapela Hill, south-western Zimbabwe, *PloS one*, *9* (10), e111224.

Chirikure, S., Mukwende, T., Moffett, A. J., Nyamushosho, R. T., Bandama, F., and House, M. 2017, No big brother here: heterarchy, Shona political succession and the relationship between Great Zimbabwe and Khami, southern Africa, *Cambridge Archaeological Journal*, 28(1), 1-22.

Colomban, Ph., 2003, Polymerization degree and Raman identification of ancient glasses used for jewelry, ceramic enamels and mosaics, *Journal of Non-Crystalline Solids, 180-187.*

Colomban, Ph., March, G., Mazerolles, L., Karmous, T., Ayed, N. Ennabli, A., and Slim, H., 2003, Raman identification of materials used for jewellery and mosaics in Ifriqiya, *Journal of Raman Spectroscopy*, 34, 205-213.

Coutinho, I., 2016, New insights into 17th and 18th century glass from Portugal: Study and Preservation, PhD dissertation, Faculdade de Ciências e Tecnologia, Universidade Nova de Lisboa.

Dungworth, D., 2011, The value of historic window glass, *The Historic Environment*, 2 (1), 21–48.

de Juan Ares, J., and Schibille, N., 2017, Glass import and production in Hispania during the early medieval period: The glass from Ciudad de Vascos (Toledo), *PLOS ONE*, 12(7), e0182129. https://doi.org/10.1371/journal.pone.0182129.

Francis, P., Jr., 1992. *Twenty easy steps to identifying most beads in most collections*. Lake Placid, N.Y.: Lapis Route Books.

Hall, R. N. and Neal, W. G., 1904, *The Ancient Ruins of Rhodesia.* Methuen & Co, London.

Hancock, R., Aufreiter, S., and Kenyon, I., 1996. European White Glass Trade Beads as Chronological and Trade Markers, MRS Proceedings, 462, 181-191. doi:10.1557/PROC-462-181.

Huffman, T. N., 1996, *Snakes and Crocodiles: Power and Symbolism in Ancient Zimbabwe*, Witwatersrand University Press, Johannesburg.

Hunt, A. M. W., and Speakman, R. J., 2015, Portable XRF analysis of archaeological sediments and ceramics, *Journal of Archaeological Science, 53, 626-638.*

Garlake, P. S., 1973, *Great Zimbabwe*, Thames and Hudson, London.

Gratuze, B., Soulier, I., Barrandon, JN., and Roy D., 1992, De l'origine du cobalt dans les verres, *Revue d' Archéometrie*, 16, 97–108.

Koleini, F., Prinsloo, L.C., Biemond, W.M., Colomban, Ph., Ngo, A. T., Boeyens, J., van der

Ryst, M., and van Brakel, K., 2016a, Unravelling the glass trade bead sequence from Magoro Hill, South Africa: separating pre-17th-century Asian imports from later European counterparts, *Heritage Science*, 4:43.

Koleini, F., Prinsloo, L.C., Biemond, W.M., Colomban, Ph., Nego, A., Boeyens, J., and van der Ryst, M., 2016b, Towards refining the classification of glass trade beads imported into southern Africa from the 8th to the 16th century AD, *Journal of Cultural Heritage*, 19, 435-444.

Koleini, F., Colomban, Ph., Antonites, A., and Pikirayi, I., 2017a, Raman and XRF classification of Asian and European glass beads recovered at Mutamba, a southern African Middle Iron Age site, *Journal of Archaeological Science*: *Reports*, 13, 333-340.

Koleini, F., Pikirayi, I., and Colomban, Ph., 2017b, Revisiting Baranda: a multi-analytical approach in classifying sixteenth/seventeenth-century glass beads from northern Zimbabwe. *Antiquity*, 91 (357), 751–764.

Lima, A., Medici, T., Pires de Matos, A., and Verità, M., 2012, Chemical analysis of 17th century millefiori glasses excavated in the monastery of Sta. Clara-a-Velha, Portugal: comparison with Venetian and façon-de-Venise production. *Journal of Archaeological Science*, 39 (5), 1238–1248.

Machiridza, L. H., 2005, *Setting the parameters for reconsidering the Rozvi archaeological identity in South-Western Zimbabwe: A Historical Archaeology Perspective*, BA Honours dissertation, University of Zimbabwe, Harare.

Machiridza, L. H. 2012, *Material Culture and dialectics of Identity and Power: Towards a Historical Archaeology of the Rozvi in South-Western Zimbabwe*, MA dissertation, University of Pretoria.

Machiridza, L. H. 2013, Insights into the meaning of vaNyai, Rozvi and Torwa: a historical archaeology approach to identities. In *Zimbabwean Archaeology: in the post-independence era*, Manyanga, M. and S. Katsamudanga (eds.), 199-212. Harare: SAPES Books.

Malandra, G., 1983, *I vetrai di Altare*, Cassa di Risparmio di Savona, Savona.

Mudenge, S. I. G., 1988, *A political history of the Munhumutapa*, Zimbabwe Publishing House, Harare.

Mysen, B., and Richet, P., 2005, *Silicate Glasses and Melts: Properties and Structures, Developments in Geochemistry*, Elsevier B.V., Amsterdam.

Pikirayi, I. 2001, *The Zimbabwe Culture; Origins and Decline of Southern Zambezian States.* Altamira Press, Walnut Creek.

Prinsloo, L.C., and Colomban, Ph., 2008, A Raman spectroscopic study of the Mapungubwe oblates: glass trade beads excavated at an Iron Age archaeological site in South Africa, *Journal of Raman Spectroscopy*, 39, 79-90.

Prinsloo, L.C., Tournié, A., and Colomban, Ph., 2011, A Raman spectroscopic study of glass

trade beads excavated at Mapungubwe hill and K2, two archaeological sites in southern Africa, raises questions about the last occupation date of the hill. *Journal of Archaeological Science,* 38, 3264-3277.

Randall-McIver, D., 1906, *Medieval Rhodesia*. McMillan, London.

Ricciardi, P., Colomban, Ph., Tournié, A., and Milande, V., 2009, Nondestructive on-site identification of ancient glasses: genuine artefacts, embellished pieces or forgeries?, *Journal of Raman Spectroscopy,* 40, 604-6017.

Robertshaw, P., Wood, M., Melchiorre, E., Popelka-Filcoff, R.S., and Glascock, M.D., 2010, Southern African glass beads: chemistry, glass sources and patterns of trade, *Journal of Archaeological Science,* 37, 1898-1912.

Robertshaw, P., and Wood, M., 2017, The glass beads from Ingombe Ilede, *Antiquity,* 91, 358, 1078-1084.

Robertshaw, P., Wood, M., Haour, A., Karklins, K., and Neff, H., 2014, Chemical analysis, Chronology, and context of a European glass bead assemblage from Garumele, Niger, *Journal of Archaeological Science,* 41, 591-604.

Schalm, O., Janssens, K., Wouters, H., and Caluwé, D., 2007, Composition of 12–18th century window glass in Belgium: Non-figurative windows in secular buildings and stained-glass windows in religious buildings, *Spectrochimica Acta* Part B, 62, 663–668.

Simsek, G., Casadio, F., Colomban, Ph., Bellot-Gurlet, L., Faber, K. T., Zelleke, G., Milande, V., and Moinet, E., 2014, On-site identification of early Böttger red stoneware made at Meissen using portable XRF: 1, body analysis, *Journal of the American Ceramics Society* 97, 9, 2745-2754.

Summers, R., 1971, *Ancient Ruins and Vanished Civilizations of southern Africa*. Gothic Printing, Cape Town.

Tournié A, Prinsloo LC, and Colomban Ph., 2012, Raman classification of the glass beads excavated on Mapungubwe hill and K2, two archaeological sites in South Africa. *Journal of Raman Spectroscopy*;43(4), 532–42.

Tournié, A., Ricciardi, P., and Colomban Ph., 2008, Glass corrosion mechanisms: A multiscale analysis, *Solid State Ionic*, 179, 2142-2154.

van Waarden, C., 2012, *Butua and the End of an Era, The effect of the collapse of the Kalanga state on ordinary citizens: An analysis of behaviour under stress*. Cambridge Monographs in African Archaeology 82. BAR S2420, Archaeopress, Oxford.

Velde, B., 2013, Glass compositions over several millennia in the Western World, in *Modern Methods for Analysing Archaeological and Historical Glass* (ed. K. Janssens), 67-78, Vol. I, Wiley, Chichester.

Wagner, B., Nowak, A., Bulska, E., Hametner, K., and Gunther, D., 2012, Critical assessment of the elemental composition of Corning archeological reference glasses by LA-

ICP-MS, *Analytical and Bioanalytical Chemistry*, 402 (4), 1667-1677.

Wood, M., 2008, Post-European contact glass beads from the southern African interior: A tentative look at trade, consumption and identities, in *Five hundred years rediscovered* (eds. N. Swanepoel, A. Esterhuysen, and P. Bonner), 183-196, Witwatersrand University Press, Johannesburg.

Wood, M., 2011, A glass bead sequence for southern Africa from the 8th to the 16th century AD, *Journal of African Archaeology*, 9(1), 67-84.

Wood, M., Dussubieux, L., and Robertshaw, P., 2012, The glass of Chibuene, Mozambique: new insights into early Indian Ocean trade, *South African Archaeological Bulletin*, 67 (195), 59–74.

Wood, M., Dussubieux, L., and Wadley, L., 2009, A cache of ~5000 glass beads from the Sibudu Cave Iron Age occupation, *South African Humanities, 21,* 239-261.

FIGURES AND TABLES

Figure 1 Map showing the location of the sites described in the paper.

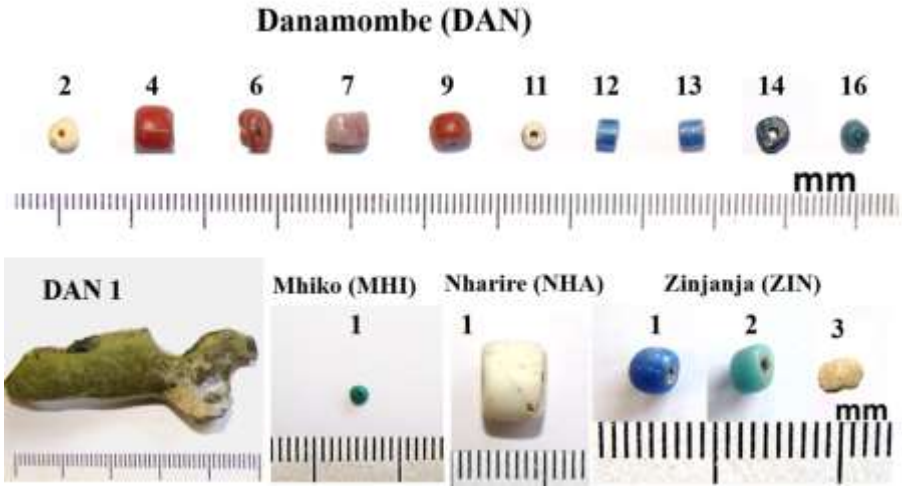

Figure 2 The beads from Danamombe, Gomoremhiko, Nharire and Zinjanja.

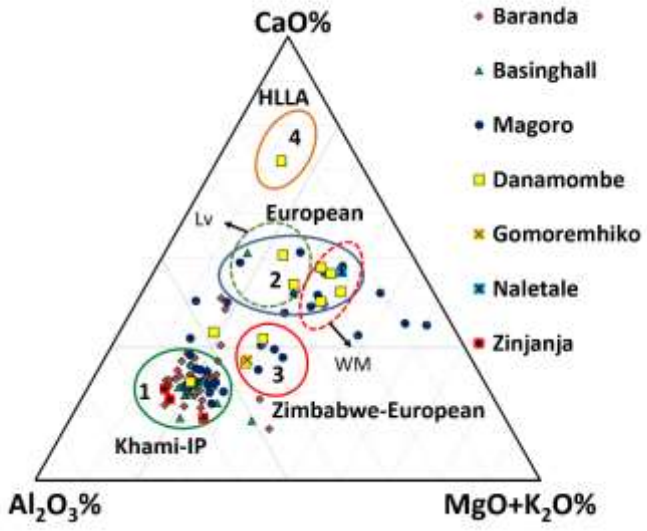

Figure 3 Ternary plot of CaO, Al_2O_3 and MgO + K_2O concentrations in glass beads from different sites in southern Africa that were analysed by pXRF (Koleini et al. 2016a, 2016b; Koleini et al. 2017b). The groups 1 to 4 are indicated. Lv: Levantine ash; WM: West Mediterranean ash

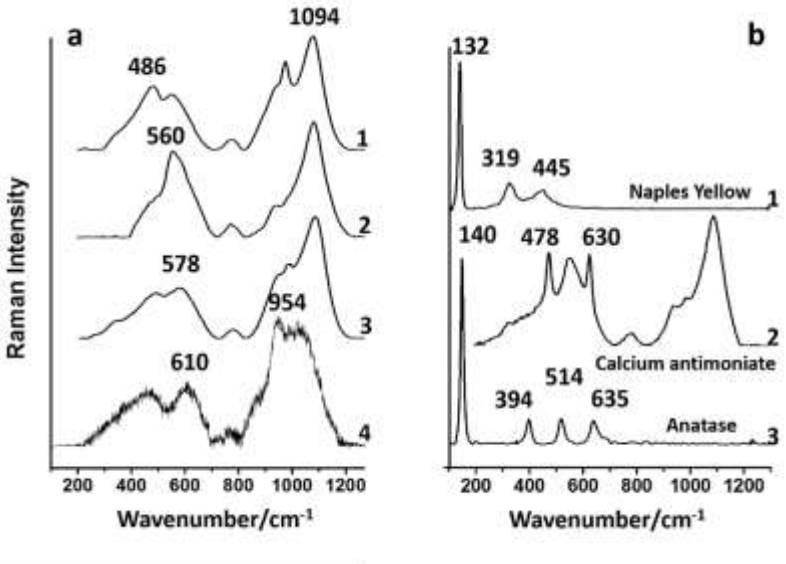

Figure 4 Representative Raman spectra after baseline correction (see Koleini et al. 2016b for procedure), a) glass matrix b) pigments; beads with the above mentioned pigments are listed in Table S4.

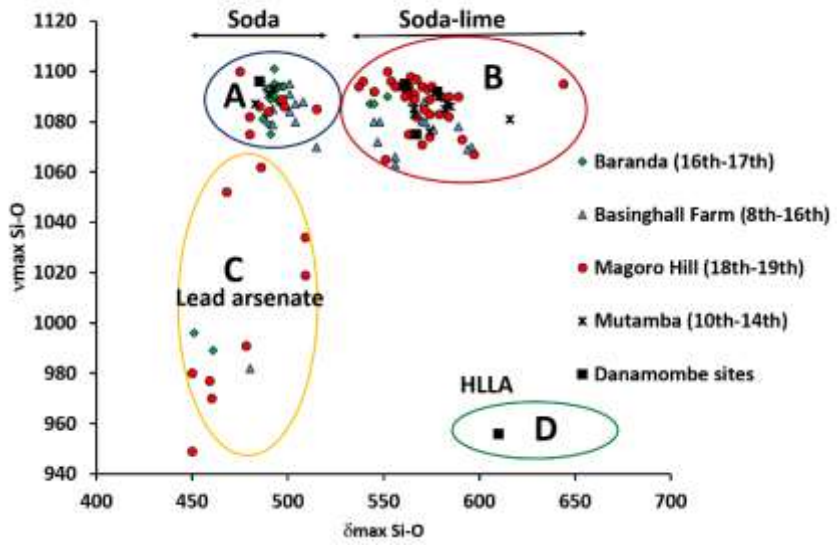

Figure 5 Plot of peak maxima in bending and stretching vibration bands of SiO_4 network.

Table 1 As measured and corrected major and minor element oxides concentration of glass beads presented in wt%

Sample	Description	MgO	Al_2O_3	SiO_2	P_2O_5	K_2O	CaO	MnO	Fe_2O_3	CoO	CuO	As_2O_3	SnO_2	Sb_2O_5	PbO	U_3O_8/ppm
DAN16	Khami	-	8.92	84.12	0.34	2.04	2.24	-	1.93	0.02	0.37	0.03	-	-	-	55
CRV*		-	7.85	68.56	0.24	2.63	3.00	-	1.83	0.02	0.41		-	-	-	-
ZIN1	Kahmi	0.87	11.91	80.26	0.41	2.91	1.85	-	1.63	0.11	-	0.05	-	-	-	121
CRV		0.84	10.48	65.41	0.28	3.75	2.48	-	1.55	0.16	-	-	-	-	-	-
ZIN2	Khami	-	14.04	77.86	0.45	2.61	2.63	-	1.99	-	0.41	-	-	-	-	57
CRV		-	12.36	63.46	0.31	3.37	3.52	-	1.89	-	0.45	-	-	-	-	-
ZIN3	Khami	-	12.35	75.18	0.53	2.01	2.60	-	1.86	-	-	-	0.82	-	4.66	48
CRV		-	10.87	61.27	0.36	2.59	3.49	-	1.76	-	-	-	0.42	-	4.89	-
DAN4	SEu-Lv	2.14	6.40	77.53	0.74	3.16	6.96	0.57	1.22	-	0.81	-	-	0.12	0.34	-
CRV		2.06	5.63	63.19	0.51	4.07	9.32	0.83	1.16	-	0.89	-	-	0.17	0.36	-
DAN6	SEu-Br	1.88	4.59	78.32	1.61	3.49	5.20	0.43	1.22	-	2.48	-	-	0.30	0.46	-
CRV		1.81	4.04	63.83	1.12	4.51	6.97	0.62	1.16	-	2.73		-	0.41	0.49	-
DAN9	SEu-Br	1.82	4.15	80.34	0.89	4.08	6.94	0.16	0.79	-	0.71	-	-	0.13	-	-
CRV		1.76	3.65	65.47	0.61	5.26	9.30	0.23	0.75	-	0.78	-	-	0.17	-	-
DAN11	SEu-Lv	1.62	6.77	74.09	0.76	3.03	8.80	0.25	1.07	-	-	-	-	3.62	0.06	-
CRV		1.56	5.95	60.38	0.53	3.91	11.79	0.36	1.01	-	-	-	-	4.89	-	-
DAN12	SEu-Br	1.57	3.99	81.88	0.74	4.68	6.11	-	0.79	0.04	-	0.19	-	-	-	-
CRV		1.51	3.51	66.73	0.51	6.04	8.19	-	0.75	0.06	-	-	-	-	-	-
DAN13	SEu-Br	1.73	4.19	82.13	0.56	3.48	6.80	-	0.88	0.06	-	0.17	-	-	-	-
CRV		1.67	3.69	66.93	0.39	4.49	9.11	-	0.84	0.08	-	-	-	-	-	-
NHA1	SEu-Br	1.66	3.65	77.58	0.61	4.65	7.17	-	0.45	-	-	-	-	4.11	-	-
CRV		1.60	3.21	63.23	0.42	5.99	9.61	-	0.43	-	-	-	-	5.55	0.13	-
DAN2	Group 3	-	12.24	72.74	0.56	3.23	5.62	-	1.71	-	-	-	-	3.77	-	-
CRV		-	10.77	59.28	0.39	4.17	7.53	-	1.62	-	-	-	-	5.10	0.12	-
DAN14	Group 3	-	12.47	74.21	0.83	5.34	4.84	0.19	1.33	0.05	-	0.15	-	-	0.57	-
CRV		-	10.98	60.48	0.57	6.89	6.49	0.28	1.27	0.07	-	-	-	-	0.60	-
DAN7	Group 3	1.48	9.88	76.83	0.57	3.92	5.32	0.15	0.93	-	0.65	-	-	-	0.27	-
CRV		1.43	8.70	62.62	0.39	5.05	7.13	0.21	0.88	-	0.72	-	-	-	0.29	-

MHI1	Map or Zim	1.72	10.86	73.62	0.58	3.43	4.36	-	1.49	-	1.32	-	1.30	-	1.31	-
CRV		1.66	9.55	60.00	0.40	4.42	5.85	-	1.41	-	1.45	-	0.66	-	1.38	-
DAN1	SEu-HLLA	2.31	5.80	69.02	2.01	1.54	17.88	0.25	1.17	-	-	-	-	-	-	-
CRV		2.23	5.11	56.26	1.38	1.99	23.96	0.37	1.11	-	-	-	-	-	-	-

*CRV= Corrected value with the impact of average normalization factors (NF) of Corning samples A and D; underline shows the oxide acting as colorant.
SEu= South European glass, Map= Mapungubwe series, Zim= Zimbabwe series Lv= Levantine ash, Br= Barilla ash

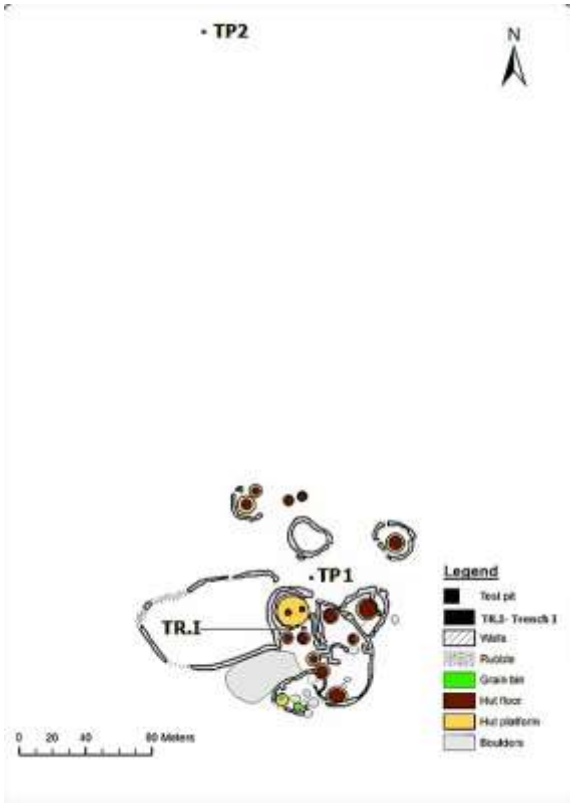

Figure S1 Danamombe site plan showing position of excavation units.

Table S1 Wood's morphological classification for southern Africa bead series (Wood 2011, 2012)

Bead series	Period traded in southern Africa	Method of manufacture	Size	Colour	Shape	Composition
Chibuene	AD 7-10th c.	Drawn	Small-medium 2.5-4.5 mm diameter	Greyish Blue, blue-green, green, yellow	Vary- most are tube and cylinder	Plant-ash lAl-lCa
Zhizo	AD 8-mid-10th	Drawn	Small-medium 2.5-4.5 mm diameter 0.7-25mm long	Dark blue, blue-green, yellow, green	Tubes	Plant-ash lAl-hCa
K2-IP	ca. AD 980-1200	Drawn	Minute-small 2-3.5 mm diameter 1.2-4 mm long	Transparent to translucent blue-green to light green	Tubes	Soda-alumina
EC-IP	ca. AD 1000-1250	Drawn	Minute- large 2-5 mm diameter	opaque black and brownish-red; yellow, soft orange, green and blue-green are translucent	Vary - most are cylindrical	Soda-alumina
Map Oblate	ca. AD 1240-1300	Drawn, Heat rounded	Minute-small 2-3.5 mm diameter	Translucent blue-green, dark blue, yellow, orange and plum. Opaque black the most common	Uniform oblates	Plant-ash hAl-lCa
Zimbabwe	ca AD 1300-1430	Drawn	Minute-small 2-3.5 mm diameter	Translucent blue-green, blue, yellow; transparent dark green, opaque black	Cylinders and oblates	Plant-ash hAl-lCa
Khami-IP	ca.AD 1430-1650	Drawn	Medium-large 3.5-5.5 mm diameter	Opaque black, brownish-red; translucent blue-green, green, yellow, orange, blue and white	Vary - most are irregular cylinders	Soda-alumina

Table S2 Report on XRF results of the main oxides (wt%) that act as glass former, stabilizer and flux in some K2, Mapungubwe, Zimbabwe and Khami series from van Riet Lowe Collection

Bead type/N	Elements	Min.	Max.	Mean	R*Min	R*Max	R*Mean
K2/2	Mg_2O	-	-	-	0.3	0.6	0.4
	CaO	1.7	1.7	1.7	2.1	2.4	2.3
	K_2O	3.9	4.2	4.0	2.8	3.2	3.0
	Al_2O_3	9.7	9.8	9.7	11.0	17.7	14.3
	Fe_2O_3	2.2	5.8	4.0	0.9	4.6	2.8
	SiO_2	78.8	82.2	80.5	60.3	61.6	61.0
	Na_2O	-	-	-	15.5	16.8	16.2
Map oblate/4	Mg_2O	2.4	3.8	3.2	4.7	5.8	5.1
	CaO	3.0	3.8	3.5	4.3	6.6	5.6
	K_2O	3.3	3.9	3.6	3.7	4.3	3.9
	Al_2O_3	6.6	9.6	8.5	8.2	10.1	9.0
	Fe_2O_3	1.4	1.8	1.6	0.7	0.9	0.8
	SiO_2	77.6	81.0	79.6	57.9	63.9	61.2
	Na_2O	-	-	-	13.5	15.5	14.3
Zimbabwe/6	Mg_2O	1.9	4.7	3.5	3.1	5.1	4.1
	CaO	4.1	4.9	4.6	5.3	8.0	7.0
	K_2O	3.5	4.1	3.7	2.9	3.9	3.3
	Al_2O_3	8.1	11.6	9.5	5.6	7.4	6.8
	Fe_2O_3	1.2	1.5	1.4	1.1	1.5	1.2
	SiO_2	74.9	79.5	77.3	60.3	67.3	63.8
	Na_2O	-	-	-	11.6	15.5	13.8
Khami/7	Mg_2O	-	1.9	0.4	0.5	2.7	1.2
	CaO	2.8	3.7	3.1	1.7	6.6	3.4
	K_2O	2.1	3.3	2.7	1.5	9.2	2.8
	Al_2O_3	8.3	12.1	9.7	5.4	16.2	9.8
	Fe_2O_3	2.1	8.2	3.7	0.8	7.3	2.7
	SiO_2	77.2	84.4	80.5	48.7	75.0	61.4
	Na_2O	-	-	-	10.4	31.8	18.7

* R= Oxides concentration of glass in the beads series based on the Robertshaw et al. 2010 measurements with LA-ICP-MS. Khami series is the result for 81 beads.
The results of pXRF in oxides form may have less accuracy than the report on elemental concentration due to the absence of sodium concentration in the main output of the instrument.

Table S3 Comparison of 19 major, minor an trace element wt% in glass references Corning B and D obtained by pXRF and LA-ICP-MS (193nm laser ablation)*

Samples	**B (mean±Std)**	**Certified value B***	**NF**	**D (mean±Std)**	**Certified value D***	**NF**
Na_2O	N/D	16.5±0.5	-	N/D	1.30±1.4	-
MgO	1.47±0.24	0.99± 0.7	0.67	3.08±1.53	3.87±1.3	1.26
Al_2O_3	5.35±0.04	4.63±1.3	0.87	5.82±0.20	5.19±3.0	0.89
SiO_2	79.71±0.19	62.02±0.3	0.78	63.66±1.95	54.15±1.2	0.85
P_2O_5	1.00±0.05	0.61±0.8	0.61	3.98±0.10	3.05±0.9	0.77
K_2O	1.06±0.03	1.30±1.4	1.22	10.42±0.21	14.2±0.7	1.36
CaO	7.05±0.13	8.75±1.4	1.24	10.19±0.23	14.7±2.4	1.44
TiO_2	0.05±0.04	0.1±1.9	2	0.24±0.01	0.36±2.7	1.5
MnO	0.17±0.03	0.24±1.2	1.4	0.42±0.05	0.60±1.1	1.5
Fe_2O_3	0.33±0.01	0.3±1.5	0.91	0.47±0.06	0.46±2.1	0.99
CoO	0.04±0.00	0.04±0.8	1	0.01±0.00	0.018±1.3	1.8
CuO	2.61±0.07	2.82±1.7	1.1	0.34±0.05	0.37±1.6	1.1
ZnO	0.18±0.01	0.21±1.7	1.17	0.08±0.01	0.1±1.6	1.25
SrO	0.01±0.00	0.02±1.9	2	0.04±0.00	0.06±2.6	1.5
Ag_2O	0.02±0.00	-	-	0.01±0.00	-	-
SnO_2	0.05±0.00	0.02±0.9	0.4	0.13±0.01	0.08±1.9	0.62
Sb_2O_5	0.35±0.01	0.42±1.8	1.2	0.64±0.05	0.96±1.9	1.5
BaO	0.08±0.00	0.08±2.5	1	0.24±0.02	0.29±1.8	1.21
PbO	0.48±0.01	0.53±2.5	1.1	0.23±0.02	0.24±1.4	1

Note: *The values available in (Wagner *et al*. 2012), NF: Normalisation factor

Table S4 The beads archaeological context, morphology, origin and estimate dates of trade

Ctx.	Lv.	Site/ID	Shape	Size	Diaphaneity	Munsell colour	Ions/Pigment	Bead Series	Assessed age (century AD)
Danamombe									
Tr. 1	4	DAN14	Oblate	Large	tsl	5.0PB 3/4-Dark blue	Co^{2+} /-	Europe	16th-8th c.
	4	DAN15	Oblate	Large	op	Charred/	-	-	-
	6	DAN17	Oblate	Medium	-	Charred/	-	-	-
	7	DAN9	Barrel	Very large	op	7.5R 3/8- Brownish-red on black	Fe^{3+}, Cu°, Mn^{2+}, Sb^{+5}/-	Europe	18^{th}-early 19th c.
	7	DAN3	Cylinder	Very large	-	Charred/	-	-	-
	7	DAN2	Oblate	Medium	op	White	$Ca_2Sb_2O_7$	Europe	late 17th to 19th c.
	8	DAN4	Barrel	Very large	op	7.5R 3/8- Brownish-red on black	Fe^{3+},Cu°, Mn^{2+}, Sb^{5+}/-	Europe	18th-early 19th c.
	8	DAN6	irregular	Large	op	7.5R 4/6-Brownish-red	Fe^{3+},Cu°, Mn^{2+}, Sb^{5+}/-	Europe	late 17th-19th c.
	8	DAN5	Oblate	Very large	opaque	Charred/	-	-	-
	10	DAN7	Cylinder	Very large	opaque	5.0R 5/6-Brownish-red on black	Fe^{3+},Cu°, Mn^{2+}/-	Europe	18th-early 19th c.
	10	DAN8	Oblate	Large	-	Charred	-	-	-
	12	DAN16	Cylinder	Medium	tsl-op	7.5B 3/3-Dark blue	Co^{2+}/-	Khami-IP	15th-17th c.
TP. 1	3	DAN1	Vessel fragment	-	tsl-trp	10.0Y 4/4 Olive	Fe^{3+}/-	Europe	16th-18th c.
TP. 2	6	DAN11	Oblate	Small	op	N8-White	$Ca_2Sb_2O_7$	Europe	late 17th-19th c.
	8	DAN13	Tube	Medium	op-tsl	5.0PB 3/6-dark blue	Co^{2+}/-	Europe	16th-18th c.
	8	DAN12	Tube	Small	op-tsl	5.0PB 3/6-Dark blue	Co^{2+}/-	Europe	16th-18th c.
Zinjanja									
TP. 2	3	ZIN1	Cylinder	Small	op	6.25PB 3/12-Dark blue	Co^{2+}/-	Khami-IP	15th-17th c.
	3	ZIN2	Cylinder	small	tsl-op	10.0B 5/6-Light blue	Cu^{2+}	Khami-IP	15th-17th c.
TP. 3	3	ZIN3	Oblate	-	op	2.5Y 9/3-Yellow	Lead tin Yellow (II)	Khami-IP	15th-17th c.
Gomoremhiko/Naletale cluster site									
TP. 1	1	MHI1	Oblate	minute	tsl-op	2.5B 5/5- Light blue	Cu^{2+}/ lead tin Yellow (II)	Zimbabwe	13th-15th c.
Nharire Hill/ Naletale cluster site									
TP. 4	2	NHA1	Cylinder	Very large	op-tsl	N9- white	$Ca_2Sb_2O_7$	Europe	late 17th-19th c.

Key: Ctx=Context, Lv.= Level, Tr.=Trench, TP.= Test Pit, tsl=translucent, trp=transparent, op=opaque

Table S5a: *List of samples submitted for radiocarbon dating and results obtained from each sample*

Direct AMS code	Submitter ID	Sample type	Fraction of modern		Radiocarbon age	
			pMC	1σ error	BP	1σ error
D-AMS024212	DANAMOMBE Sample 1	charcoal	98.96	0.38	84	31
D-AMS024213	DANAMOMBE Sample 2	charcoal	98.66	0.29	108	24
D-AMS024214	DANAMOMBE Sample 3	charcoal	94.68	0.33	439	28
D-AMS024215	DANAMOMBE Sample 4	charcoal	97.72	0.4	185	33
D-AMS024216	DANAMOMBE Sample 5	charcoal	Failed in analysis			
D-AMS024217	NALETALE Sample 1	charcoal	97.67	0.37	189	30
D-AMS024218	NALETALE Sample 2	charcoal	97.90	0.27	170	22
D-AMS024219	NALETALE Sample 3	charcoal	98.13	0.36	152	29
D-AMS024220	ZINJANJA Sample 1	charcoal	98.54	0.36	118	29
D-AMS024221	ZINJANJA Sample 2	charcoal	98.83	0.32	95	26

Results are presented in units of percent modern carbon (pMC) and the uncalibrated radiocarbon age before present (BP). All results have been corrected for isotopic fractionation with an unreported δ13C value measured on the prepared carbon by the accelerator. The pMC reported requires no further correction for fractionation.

Table S5b: *A detailed summery of calibrated dates from the three research sites*

Dates from Danamombe Trench I, Main Platform and Test Pit II, Midden						
Context/matrix description	**Level**	**BP**	**2 Sigma Age ranges**	**Relative error Under Probability**	**1 Sigma Age ranges**	**Relative error Under Probability**
Trench I Main platform: Burnt ashy layer lying just below the first four hut floors but resting on closely packed granite blocks	5 (40-50 cm)	84 +/- 31	1686-1731 1808-1927	0.269 0.731	1696-1725 1814-1836 1845-1848 1877-1917	0.303 0.216 0.024 0.457
Trench I Main platform: Heavily burnt ashy layer extending from well packed blocks but situated above hut floor 5	11-12 (110-120 cm)	108 +/- 24	1683-1734 1806-1929	0.287 0.713	1694-1713 1716-1727 1813-1854 1857-1863 1866-1891 1909-1918	0.181 0.105 0.304 0.044 0.236 0.094
Trench I Main platform: Large packed blocks lying just under hut floor 6 with signs of heavy burning on its floor surface	16 (150-160cm)	439 +/- 28	1420-1486	1.000	1433-1457	1.000
Test Pit II/ Midden 300m away from platform: Fine textured ashy layer	7 (60-70cm)	185 +/- 33	1649-1696 1725-1814 1836-1845 1850-1876 1917-1950	0.222 0.557 0.011 0.030 0.180	1665-1682 1736-1786 1792-1805 1935-1950	0.197 0.516 0.121 0.166
Dates from Naletale Test Pit II, Main Platform						
Test Pit II Naletale Main platform: Compacted gritty reddish brown soil just above hut floor 1	2 (10-20 cm)	152 +/- 29	1667-1708 1718-1783 1796-1827 1831-1887 1911-1950	0.172 0.348 0.120 0.177 0.182	1670-1694 1727-1779 1798-1813 1839-1841 1854-1857 1862-1866 1918-1950	0.191 0.444 0.115 0.005 0.017 0.023 0.205

Test Pit II Naletale Main platform: Reddish brown layer just below hut floor 1 but extending into packed granite blocks	6-7 (50-70cm)	170 +/- 22	1664-1694 1727-1813 1839-1841 1854-1857 1863-1866 1918-1950	0.186 0.610 0.001 0.003 0.002 0.197	1669-1683 1736-1780 1798-1805 1934-1945	0.172 0.598 0.091 0.139
Test Pit II Naletale Main platform: Neatly packed stones just below hut floor 3, these blocks were laid on bedrock	12-13 (110-130cm)	189 +/- 30	1649-1694 1727-1813 1839-1841 1854-1857 1863-1866 1918-1950	0.234 0.580 0.001 0.002 0.002 0.181	1664-1681 1738-1755 1762-1787 1791-1803 1937-1950	0.212 0.172 0.314 0.127 0.176
Dates from Zinjanja Test Pit II and Test Pit III Midden area						
Zinjanja Test Pit II/ Midden 200m away from Main platform: Grey compacted soil extending into a sterile layer	7 (60-70cm)	118 +/- 29	1680-1739 1742-1763 1802-1938	0.285 0.042 0.672	1687-1709 1717-1730 1809-1828 1831-1889 1910-1926	0.164 0.095 0.145 0.466 0.130
Zinjanja Test Pit III/ Midden 200m away from Main platform: Compact dark grey clayey soil	4 (30-40cm)	95 +/- 26	1688-1730 1809-1926	0.272 0.728	1696-1726 1814-1836 1844-1851 1869-1872 1876-1898 1901-1917	0.312 0.234 0.051 0.025 0.215 0.163

Table S5c: *Additional samples submitted for radiocarbon dating and results obtained from each*						
Direct AMS code	**Submitter ID**	**Sample type**	**Fraction of modern**		**Radiocarbon age**	
			pMC	**1σ error**	**BP**	**1σ error**
D-AMS025194	DANAMOMBE Sample 1	charcoal	98.98	0.41	82	33
D-AMS025195	DANAMOMBE Sample 2	charcoal	98.33	0.34	135	28
D-AMS025196	DANAMOMBE Sample 3	charcoal	95.13	0.38	401	32
D-AMS025197	DANAMOMBE Sample 4	charcoal	99.09	0.22	74	18

Table S5d: *A detailed summary of calibrated dates for Danamombe additional samples*						
Dates from Danamombe Trench I, Main Platform and Test Pit II, Midden						
Context/matrix description	**Level**	**BP**	**2 Sigma Age ranges**	**Relative error Under Probability**	**1 Sigma Age ranges**	**Relative error Under Probability**
Trench I Main platform: Burnt ashy layer lying just below the first four hut floors but resting on closely packed granite blocks	40-50 (4-5 cm)	82 +/- 33	1685-1732 1808-1928	0.270 0.730	1696-1725 1814-1836 1845-1850 1877-1917	0.297 0.212 0.039 0.452
Trench I Main platform: Heavily burnt ashy layer extending from well packed blocks but situated above hut floor 5	11-12 (110-120 cm)	135 +/- 28	1673-1778 1799-1892	0.424 0.418	1681-1699 1721-1739 1744-1763 1802-1818 1833-1879 1915-1938	0.141 0.131 0.107 0.116 0.335 0.171
Trench I Main platform: Large packed blocks lying just under hut floor 6 with signs of heavy burning on its floor surface	16 (150-160cm)	401 +/- 32	1435-1522 1573-1628	0.785 0.215	1443-1493 1602-1613	0.872 0.128
Trench I Main platform: Artificial platform of large and small packed blocks mixed with loose gritty soil	21 (200-210cm)	74 +/- 18	1696-1726 1813-1838 1842-1853 1868-1918	0.237 0.168 0.027 0.568	1707-1719 1820-1821 1825-1832 1884-1913	0.194 0.010 0.102 0.694

Table S6 Southern Europe high alumina glass (Al_2O_3>3.5%)

Glass type	Soda rich plant ash (Group2)	Soda rich plant ash (Group 2)	HLLA (Group 4)
Ashes	Levantine ash (K_2O<4%)	Barilla ash (K_2O>4.5%)	Wood ash
Date	AD 10-17th c.	AD 13-19th c.	AD 15-18th c.
Locations in Europe	Savona (10-16th c.), Tuscan (13-16th c.) Vascos (10-12th c.), Silves (11-13th c.) Coimbra (17th c.), Tarouca Monastery (17th c.)	Savona (13-16th c.), Tuscan (mid-16th c.), Coimbra (17th c.)	Savona (15-16thc.)
Analysed beads	DAN4, DAN11	DAN6, DAN9, DAN12, DAN13,	DAN1

References: Cagno et al. (2012), Cagno et al. (2010), Coutinho (2016), de Juan Ares and Schibille (2017), Velde 2013